Manuscript Title: Investigating the roles of visual and parietal cortex in representing content versus context in visual working memory

Abbreviated title:

Neural basis of content versus context in working memory

Authors:

Chunyue Teng[1], Bradley R. Postle[1,2]

Affiliations:

[1]Department of Psychiatry, University of Wisconsin–Madison, Madison, WI 53719, USA

[2]Department of Psychology, University of Wisconsin–Madison, Madison, WI 53706, USA

Author contributions:

C.T. and B.R.P. designed research; C.T. and B.R.P. wrote the paper.

***Correspondence should be addressed to:**

Bradley R. Postle

Department of Psychology

University of Wisconsin-Madison

Madison, WI 53706, USA

Email: postle@wisc.edu

Number of Figures: 2

Number of words for Abstract: 212

Number of words for Significance Statement: 124

Number of words for Introduction: 757

Acknowledgements: This work is supported by National Institutes of Health grant R01MH064498 (to B.R.P.).

Conflict of Interest: Authors report no conflict of interest.

Abstract

Successful working memory performance requires the binding of contextual cues to item-related content. In a recent study that used a dual-serial retrocueing (DSR) procedure to test working memory for oriented gratings, the unprioritized memory item (UMI) underwent a representational transformation – a priority-based remapping – of the representation of its orientation (i.e., its content) in early visual cortex, and of the representation of the location at which it had been presented (i.e., its context) in parietal cortex (Yu, Teng, & Postle, in press). In this registered report, we will scan healthy adults with functional magnetic resonance imaging (fMRI) while they perform a DSR task with the roles of content and context reversed: stimulus location will be the to-be-reported content and stimulus orientation the task-relevant context. We will use multivariate inverted encoding modeling (IEM) to test between three models of the neural bases of the priority-based remapping of stimulus information: 1) *domain-dependent* -- the engagement of early visual and parietal regions in priority-based remapping depends on domain of information (orientation versus location) – 2) *functional* -- the engagement of these regions in priority-based remapping will depend depends on function (content versus context); 3) *hybrid*: predictions follow the domain-dependent model, but with the additional stipulation that IPS plays a critical role in representing context, regardless of domain.

Significance Statement

The binding between the content of working memory and the context in which that information was encountered is of critical importance for guiding behavior with remembered information. When attention is shifted away from a stimulus held in working memory, the representation of its content and of its context are transformed, but in different brain areas. This preregistered report is designed to understand the principal factor underlying this dissociation: is it that different regions are specialized for representing different domains of content (e.g., an item's orientation versus its location); that different regions are specialized for different working memory functions (i.e., representing content versus context); or some hybrid combination of these two? The results will provide important insights into the mechanisms that support visual working memory.

Introduction

The retention of information in visual working memory entails the binding of item-related information – the to-be-remembered content – with its trial-unique context (e.g., spatial location or the ordinal position). Furthermore, it has been proposed that the strength of this content-to-context binding may be an important determinant of the precision of a memory representation (Oberauer and Lin, 2017). Although several studies have assessed the neural representation of to-be-remembered stimulus features (e.g., Emrich et al., 2013; Harrison and Tong, 2009; Riggall and Postle, 2012; Sprague and Serences, 2013), the representation of context has received less attention (c.f., Foster et al., 2017; Gosseries, Yu et al., 2018). The current study is designed to assess whether the brain represents the same information differently when it serves as working memory context, rather than content.

In a recent experiment, Yu, Teng, and Postle (in press) assessed the representation of content and of context in visual working memory with functional magnetic resonance imaging (fMRI). In a dual-serial retrocueing (DSR) task, two sample orientation gratings were presented sequentially in one of nine possible locations, then an ordinal retrocue ("1" or "2") indicated the sample whose orientation would need to be reported for the first impending recall. After the first recall, subjects perform the second recall based on a second retrocue. Prior to the first retrocue, using multivariate inverted encoding modeling (IEM), the orientation of both sample stimuli could be reconstructed in early visual cortex, and their locations in early visual cortex and intraparietal sulcus (IPS). The first retrocue then designated the cued item the "prioritized memory item" (PMI) and the uncued item the "unprioritized memory item" (UMI), and the transition to UMI triggered distinctive changes in its representational format. In early visual cortex, the reconstruction of the UMI's orientation became opposite of its reconstruction as a

PMI, whereas in IPS, the reconstruction of the UMI's location shifted to become opposite of its reconstruction as a PMI. Importantly, these reported priority-based transformations were characterized as examples of remapping between the stimulus values and the neural patterns, not of recoding (Yu et al., in press), because they were reconstructed with IEMs trained on the PMI.

This phenomenon of "priority-based remapping" has also been observed in EEG data from (Wan et al., in-principle accepted registered report) and in computational simulations of (Wan et al., 2019) a 2-back working memory task. In the present paper, we will use it as a tool to test competing models of the neural representation of content versus context in visual working memory. The results from Yu et al. (in press) are equally consistent with at least three interpretations. One is that neural loci of the representation of an item's content and of its context are domain dependent. By this account, early visual cortex carries a privileged role in representing orientation and IPS carries a privileged role in representing retinotopic location. An alternative interpretation, however, is a functional account: Early visual cortex may be preferentially involved in representing an item's content, and IPS in representing an item's context. This alternative view would be consistent with evidence for IPS sensitivity to context binding demands when task-critical context is ordinal position, and location doesn't vary (Gosseries, Yu., et al., 2018). A third possibility is a hybrid view that ascribes to the domain-dependent processing of orientation in early visual cortex and of location in IPS, but that also posits an important functional role for IPS in representing the context of information, regardless of domain. This view would be consistent with findings of retinotopic maps in parietal cortex (e.g. Sereno et al., 2001; Silver et al., 2005) and with evidence for IPS's involvement in context-binding with ordinal context (Gosseries, Yu., et al., 2018).

The purpose of the present study is to compare among the three interpretations of the results from Yu et al. (in press), by switching the roles played by stimulus orientation and location. Subjects will perform a DSR task in which the two sample stimuli are each distinguished by their location and their orientation, but the subject's task is explicitly to recall stimulus location (Figure 1). The item to be recalled for each memory probe will be retrocued by its orientation. Thus, stimulus location will serve as the content and stimulus orientation as the context. Priority-based remapping during the delay period following the first retrocue will be operationalized by a negative slope of the reconstruction of a stimulus dimension of the UMI during the final TR of the post-cue delay, with an IEM trained on that same TR during trial epochs when that item was the PMI.

Materials and Methods

Pre-registered hypotheses

In this section, for each of the following results that our study is designed to generate, we specify what each of the three models predicts for the IEM reconstruction of stimulus information in two functionally defined regions of interest (ROI; these predictions are illustrated in Figure 2):

Content of PMI in early visual cortex:

All three models assume that the reconstruction of the location of the PMI with a PMI-trained model will have a significantly positive slope, a replication of Yu et al. (in press).

Context of PMI in early visual cortex:

Domain-dependent: The reconstruction of the orientation of the PMI with a PMI-trained model will have a significantly positive slope.

Functional: The reconstruction of the orientation of the PMI with a PMI-trained model will not differ from 0.

Hybrid: The reconstruction of the orientation of the PMI with a PMI-trained model will have a significantly positive slope.

Content of UMI in early visual cortex:

Domain-dependent: The reconstruction of the location of the UMI with a PMI-trained model will not differ from 0.

Functional: The reconstruction of the location of the UMI with a PMI-trained model will have a significantly negative slope.

Hybrid: The reconstruction of the location of the UMI with a PMI-trained model will not differ from 0.

Context of UMI in early visual cortex:

Domain-dependent: The reconstruction of the orientation of the UMI with a PMI-trained model will have a significantly negative slope.

Functional: The reconstruction of the orientation of the UMI with a PMI-trained model will not differ from 0.

Hybrid: The reconstruction of the orientation of the UMI with a PMI-trained model will have a significantly negative slope.

Content of PMI in IPS:

Domain-dependent: The reconstruction of the location of the PMI with a PMI-trained model will have a significantly positive slope.

Functional: The reconstruction of the location of the PMI with a PMI-trained model will not differ from 0.

Hybrid: The reconstruction of the location of the PMI with a PMI-trained model will have a significantly positive slope.

Context of PMI in IPS:

Domain-dependent: The reconstruction of the orientation of the PMI with a PMI-trained model will not differ from 0.

Functional: The reconstruction of the orientation of the PMI with a PMI-trained model will have a significantly positive slope.

Hybrid: The reconstruction of the orientation of the PMI with a PMI-trained model will have a significantly positive slope.

Content of UMI in IPS:

Domain-dependent: The reconstruction of the location of the UMI with a PMI-trained model will have a significantly negative slope.

Functional: The reconstruction of the location of the UMI with a PMI-trained model will not differ from 0.

Hybrid: The reconstruction of the location of the UMI with a PMI-trained model will have a significantly negative slope.

Context of UMI IPS:

Domain-dependent: The reconstruction of the orientation of the UMI with a PMI-trained model will not differ from 0.

Functional: The reconstruction of the orientation of the UMI with a PMI-trained model will have a significantly negative slope.

Hybrid: The reconstruction of the orientation of the UMI with a PMI-trained model will have a significantly negative slope.

Subjects

Estimated effect sizes for this preregistered study are based on data sets from Yu et al. (in press) that used data collection and analysis methods similar to what we will use for this preregistered study. Power analyses indicate we will need data from 24 subjects to achieve 90% power to detect the smallest of the predicted significant effects (significantly negative slope for the reconstruction of orientation of the UMI in early visual cortex, Cohen's d of 0.62) with a one-tailed alpha of 0.05.

Male and female subjects will be recruited at a location which will be identified if the article is published with the following inclusion criteria: being 18-35 years in age, having normal or corrected-to-normal vision, reporting no history of neurological disease, seizures, or fainting, no history of using of psychotropic drugs nor of chronic alcohol consumption, and having no contraindications for MRI scanning. Informed consent will be obtained following procedures approved by the [Author University] Health Sciences Institutional Review Board.

Stimuli and procedure

The stimuli used in the task will be generated with MATLAB (MathWorks) and the Psychtoolbox-3 extensions and presented with a 60-Hz Avotec Silent Vision 6011 projector (Brainard, 1997; Pelli, 1997). Subjects will view the stimuli through a coil-mounted mirror, with a viewing distance of 68.58 cm and the screen width of 33.02 cm. The stimuli during the sample period will be two oriented bars colored black (length 5°, width 0.08; presented inside a white disk of radius of 2.5°). The orientation of the two bars will be selected randomly, without replacement, from a fixed set of values (15°, 45°, 75°, 105°, 135°, or 165°; approximately 54 instances of each). The locations of the disks will be selected randomly, without replacement, from fixed a set of nine values of polar angle (20°, 60°, 100°, 140°, 180°, 220°, 260°, 300°, 340°; approximately 36 instances of each), each centered on an imaginary circle with a radius of 8° from central fixation. In order to cover the 360° space and avoid verbal encoding, on each trial, a jitter between 0° to 10° will be added to both sample locations with the same value. There will be six possible distances between the PMI and UMI in orientation space: -60°, -30°, 0°, 30°, 60°, and 90°; and nine possible distances between the PMI and UMI along the imagery circle: -160°, -120°, -80°, -40°, 0°, 40°, 80°, 120°, and 160°. Distance in location, distance in orientation, and status of the second retrocue (stay/switch) will be fully counterbalanced, resulting in 108 unique trial types. This design means that the orientation of the two samples will be the same on a fixed proportion of 1/6th of trials, and the location samples will be the same on a fixed proportion of 1/9th of trials. Responses will be collected with an MRI-compatible button box.

Subjects will be scanned while performing working memory for locations in a DSR task (Figure 1). Each trial will begin with the 2 second presentation of two sample stimuli, followed by an initial delay period of 8 seconds (Delay 1.1). At time 10-seconds a retrocue will present (for 2 seconds) the orientation of the item whose location will be probed at the end of an addition 8 second-long delay period (Delay 1.2). In order to avoid differential sensory presentation of the two orientations, the retrocue will contain two bars, one red and one blue, that correspond to the orientation of the two samples, and one of the colors (counterbalanced across subjects) will designate the valid cue. Subjects will be told the color of the valid cue at the beginning of the experiment. The recognition probe will be a white disk (radius of 2.5°) presented for 2.5 seconds at a location that matches the location of the cued item on 50% of trials, and at a location with varying distances from that of the cued item on nonmatching trials (15°, 25°, or 35°, counterbalanced across trials). Probe offset will be followed by a 1-second unfilled delay (Delay

2.1), a second retrocue (2 seconds), two additional seconds of delay (Delay 2.2), and a second memory probe. The second retrocue will be identical to the first, unpredictably, on 50% of trials ("stay" trials), and will cue the previously uncued item on 50% of trials ("switch" trials). A white fixation dot will be present throughout the trial except when replaced by the retrocues. The inter-trial interval will vary randomly between 6, 8, and 10 seconds.

Over the course of two scanning sessions subjects will perform a total of 324 trials (3 of each unique type). The first scanning session will consist of 13 runs during each of which a block of 12 trials will be performed, and the second scanning session will consist of 14 run/blocks. Each run/block will last 464 seconds. Before the first scanning session, each subject will complete two blocks of practice trials (12 trials per block) outside of the scanner and another block of practice within the scanner before fMRI scanning begins. During the fMRI scans, we will track subjects' eye position using an Avotec RE-5700 eye-tracking system, to monitor central fixation.

Behavioral data analysis

We will first derive a descriptive measure of each subject's performance during Probe 1 and Probe 2 by calculating the percentage of correct responses and the average response time. We will compare the accuracy between Probe 1 and Probe 2 and compare the performance for *stay* and *switch* trials.

fMRI Data acquisition

Whole brain images will be acquired with a 3-T MRI scanner (Discovery MR750; GE Healthcare) at the [Author University]. A high-resolution T1-weighted image will be acquired with a fast-spoiled gradient-recalled echo sequence (repetition time (TR) of 8.2 ms, echo time (TE) of 3.2 ms, flip angle of 12°, 176 axial slices, 256 x 256 in-plane, 1.0 mm isotropic). A T2*-weighted gradient echo pulse sequence will be used to acquire the functional data while subjects perform the DSR task (TR of 2 s; TE of 25 ms; flip angle of 60°; 64 x 64 matrix size, 42 sagittal slices, 3 mm isotropic).

fMRI Preprocessing

Data will be preprocessed using the Analysis of Functional Neuroimages (AFNI) software package (https://afni.nimh.nih.gov). Before statistical analysis, the data will be first registered to the final volume of each scan with rigid-body transformations and then to the anatomical images of the first scan session, after removing the first four TRs at the beginning of each run (dummy pulses to achieve a steady state of tissue magnetization before task onset). Then volumes will be motion corrected with six nuisance regressions accounting for motion artifacts in six different directions. Linear, quadratic, and cubic trends will be removed for each run and then the data will be z-scored within each run.

Region of interest (ROI) generation

As with Yu et al. (in press), we will focus the analyses on two functionally defined and anatomically constrained ROIs: early visual ROI (constrained to V1 and V2 in occipital cortex) and IPS (constrained to IPS0-5). Anatomical ROIs will be generated from the probabilistic atlas of (Wang et al., 2015) and warped to each subject's structural scan in their native space. To identify voxels maximally engaged by the task, we will fit the fMRI data to a general linear model (GLM) containing regressors for each epoch of the task -- sample (1-TR impulse), delay

1.1 (8-s boxcar), cue 1 (1-TR impulse) delay 1.2 (8-s boxcar), probe 1 (1-TR impulse), delay 2 (1-TR impulse), and probe 2 (1-TR impulse), each convolved with a hemodynamic response function -- along with nuisance covariates for between-scan drift and head motion. Within each anatomically defined region, the functional ROIs will be defined as the 500 voxels with the strongest values for the sample regressor within the early visual ROI, and the 500 voxels with the strongest values for the delay 1.2 regressor within IPS.

Inverted encoding model

Multivariate inverted encoding models (Brouwer and Heeger, 2011, 2009; Ester et al., 2015; Yu and Shim, 2017) will be used to reconstruct the neural representation of PMIs and UMIs. The responses of each voxel can be modeled as a weighted sum of responses from a number of hypothetical tuning channels. We will use nine tuning channels for location reconstruction and six channels for orientation reconstructions. The idealized tuning curve of each channel was defined as a half-wave-rectified sinusoid raised to the eighth power for location: $R = \sin^8(x)$, and to the sixth power for orientation: $R = \sin^6(x)$, where *x* is the centered on the orientation or location this channel is mostly selective to and *R* is the channel response.

For the IEM, we first estimate an encoding model with a training dataset B_1 (v voxels × n trials) to characterize each voxel's selectivity $\widehat{\boldsymbol{W}}$ (v voxels × k channels) for the feature dimension. Then we input a new dataset B_2 (v voxels × n trials) with all the voxels' responses on a single trial to the model to reconstruct a model-based representation of memorized orientation or location C_2. We can first describe the data with the following equation:

$$\boldsymbol{B}_1 = \boldsymbol{W}\boldsymbol{C}_1$$

Here B_1 represents the data matrix of BOLD responses with a size of $v \times n$ for each run where v is the number of voxels in the ROI and n is the number of trials. C1 is the idealized responses of each tuning channel for each trial (k channels × n trials). W (v voxels × k channels) is the weight matrix that captures the selectivity of each voxel for orientations or locations.

The first step of the IEM is to train the IEM on the training dataset B_1 and compute the weight matrix $\widehat{\boldsymbol{W}}$ that contains each voxel's selectivity at each orientation or location channel with least-squares linear regression:

$$\widehat{\boldsymbol{W}} = \boldsymbol{B}_1 \boldsymbol{C}_1^T (\boldsymbol{C}_1 \boldsymbol{C}_1^T)^{-1}$$

The next step is to invert the model with the estimated weight matrix and a new test dataset B_2 (v voxels × n trials) to derive the reconstructed channel responses C2 (k channels × n trials) for each trial with the following equation:

$$\widehat{\boldsymbol{C}_2} = (\widehat{\boldsymbol{W}}^T \widehat{\boldsymbol{W}})^{-1} \widehat{\boldsymbol{W}}^T \boldsymbol{B}_2$$

With this procedure, we can compute a trial-by-trial reconstruction of the maintained orientation and location for PMIs and UMIs.

The IEMs will be trained and tested separately for orientation and location, and separately for the early visual ROI and IPS ROI. We will use a leave-one-out procedure that will train the model with data from all but one run and test the model on the one run that is left out. We will repeat this process until we compute the channel responses for all the runs. The IEMs will be trained and tested on the same TR. Although we will examine the time courses of IEM reconstructions from task onset until the beginning of Probe 1 (0 to 22 s), our hypotheses about priority-based changes in the neural representations of the UMI will focus on one TR: TR 10, the final TR of Delay 1.2 (based on the findings in Yu et al., in press). For the PMI-trained IEMs, the training labels will be based on orientation or location of the PMI. After generating the reconstruction for each trial, the estimated channel responses will be shifted to a common center, with 0° as the test orientation channel. Overall, we will generate reconstruction of PMIs and UMIs in the two ROIs based on the PMI-trained model.

fMRI Statistical analysis

We will quantify the strength of the neural reconstructions by collapsing over channel responses on both sides of the target channel (0° center), averaging them, and then use linear regression to calculate the slope for the reconstruction for each subject. A positive slope will be interpreted as evidence that the dimension of sample-related information in question (location or orientation) is encoded in the same format as was the data the model was trained on. A negative slope will be interpreted as evidence that the dimension of sample-related information in question (location or orientation) is encoded in a format that is remapped relative to the data the model was trained on. The magnitude of the slope will be interpreted as the precision of the reconstructed neural representation. For statistical testing, we will use a bootstrapping method (Ester et al., 2016, 2015) in which we will randomly sample with replacement 24 reconstructions (corresponding to N = 24 subjects) and take the average of the resulting channel responses, repeating this process 10000 times. This will result in 10000 average orientation/location reconstructions with 10000 slopes computed for the reconstructions. For the statistical testing, we will compute two-tailed p-values as the smaller of two resultant values – the proportion of positive slopes or the proportion of negative slopes – multiplied by 2. To compare the difference between the slopes of PMI and UMI, we will randomly sample with replacement to create a sample of 24 subjects and compute the difference in slope between PMI and UMI, repeating this process 10000 times, and will then assess significance with the same procedure as described above.

Timeline

Data collection will begin in Fall 2020 and is expected to conclude by March 2021. Data processing and analysis will be carried out in parallel to data collection for each single subject. The project is expected to fully complete by May 2021.

References

Brainard DH (1997) The Psychophysics Toolbox. Spat Vis 10:433–436.

Brouwer GJ, Heeger DJ (2011) Cross-orientation suppression in human visual cortex. J Neurophysiol 106:2108–2119.

Brouwer GJ, Heeger DJ (2009) Decoding and reconstructing color from responses in human visual cortex. J Neurosci 29:13992–14003.

Emrich SM, Riggall AC, Larocque JJ, Postle BR (2013) Distributed Patterns of Activity in Sensory Cortex Reflect the Memory. J Neurosci 33:6516–6523.

Ester EF, Sprague TC, Serences JT (2015) Parietal and Frontal Cortex Encode Stimulus-Specific Mnemonic Representations during Visual Working Memory. Neuron 87:893–905.

Ester EF, Sutterer DW, Serences JT, Awh E (2016) Feature-selective attentional modulations in human frontoparietal cortex. J Neurosci 36:8188–8199.

Foster JJ, Bsales EM, Jaffe RJ, Awh E (2017) Alpha-Band Activity Reveals Spontaneous Representations of Spatial Position in Visual Working Memory. Curr Biol 27:3216–3223.

Gosseries O, Yu Q, Larocque JJ, Starrett MJ, Rose NS, Cowan N, Postle BR (2018) Parietal-occipital interactions underlying control-and representation-related processes in working memory for nonspatial visual features. J Neurosci 38:4357–4366.

Harrison SA, Tong F (2009) Decoding reveals the contents of visual working memory in early visual areas. Nature 458:632–635.

Oberauer K, Lin HY (2017) An interference model of visual working memory. Psychol Rev 124:21–59.

Pelli DG (1997) The VideoToolbox software for visual psychophysics: Transforming numbers into movies. Spat Vis 10:437–442.

Riggall AC, Postle BR (2012) The Relationship between Working Memory Storage and Elevated Activity as Measured with Functional Magnetic Resonance Imaging. J Neurosci 32:12990–12998.

Sereno MI, Pitzalis S, Martinez A (2001) Mapping of contralateral space in retinotopic coordinates by a parietal cortical area in humans. Science (80-) 294:1350–1354.

Silver MA, Ress D, Heeger DJ (2005) Topographic maps of visual spatial attention in human parietal cortex. J Neurophysiol 94:1358–1371.

Sprague TC, Serences JT (2013) Attention modulates spatial priority maps in the human occipital, parietal and frontal cortices. Nat Neurosci 16:1879–1887.

Wang L, Mruczek REB, Arcaro MJ, Kastner S (2015) Probabilistic maps of visual topography in human cortex. Cereb Cortex 25:3911–3931.

Wan Q, Cai Y, Samaha J, Postle BR (accepted in principle). Tracking stimulus representation across a 2-back visual working memory task. *Royal society Open Science*.

Wan Q, Cai Y, Samaha J, Rogers TT, and Postle BR (2019). Rotational remapping as a candidate mechanism for priority-based recoding in visual working memory: Empirical and computational evidence. *Society for Neuroscience,* November 2019, Chicago, IL.

Yu Q, Shim WM (2017) Occipital, parietal, and frontal cortices selectively maintain task-relevant features of multi-feature objects in visual working memory. Neuroimage 157:97–107.

Yu Q, Teng C, & Postle BR (in press). Different states of priority recruit different neural codes in visual working memory.

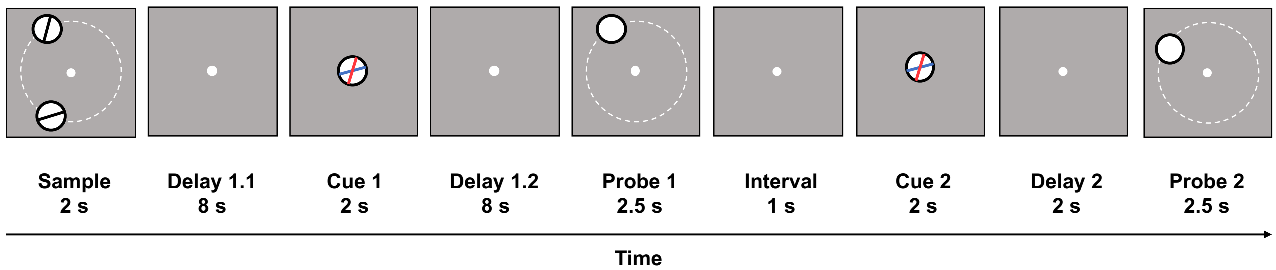

Figure 1. Procedures of the experiment. Subjects will perform a dual serial-retrocueing task on location. Two sample stimuli will be presented at nine possible locations with six possible orientations and the task will be to memorize the spatial locations of both. The white dotted circles are for illustrative purposes and will not be present during the actual experiment. The distances in orientations and locations between the two stimuli will be fully counterbalanced, such that they will match on 1/9th and 1/6th of trials, respectively. After Delay 1.1, an orientation cue (superimposed red and blue oriented bars inside a central disk) will appear with the red bar (or blue bar, counterbalanced between subjects) indicating the sample whose location is to be reported during Probe 1. Probe 1 consists of a filled white disk that will appear in a location either completely matching or slightly mismatching the location that the cued sample had occupied, and subjects will make a same/different judgement on its location. Subsequently, a second orientation cue will appear after an interval of 1 s, and subjects will respond during Probe 2 based on the red oriented bar. Each trial will be separated by an ITI jittered between 6, 8, and 10 seconds.

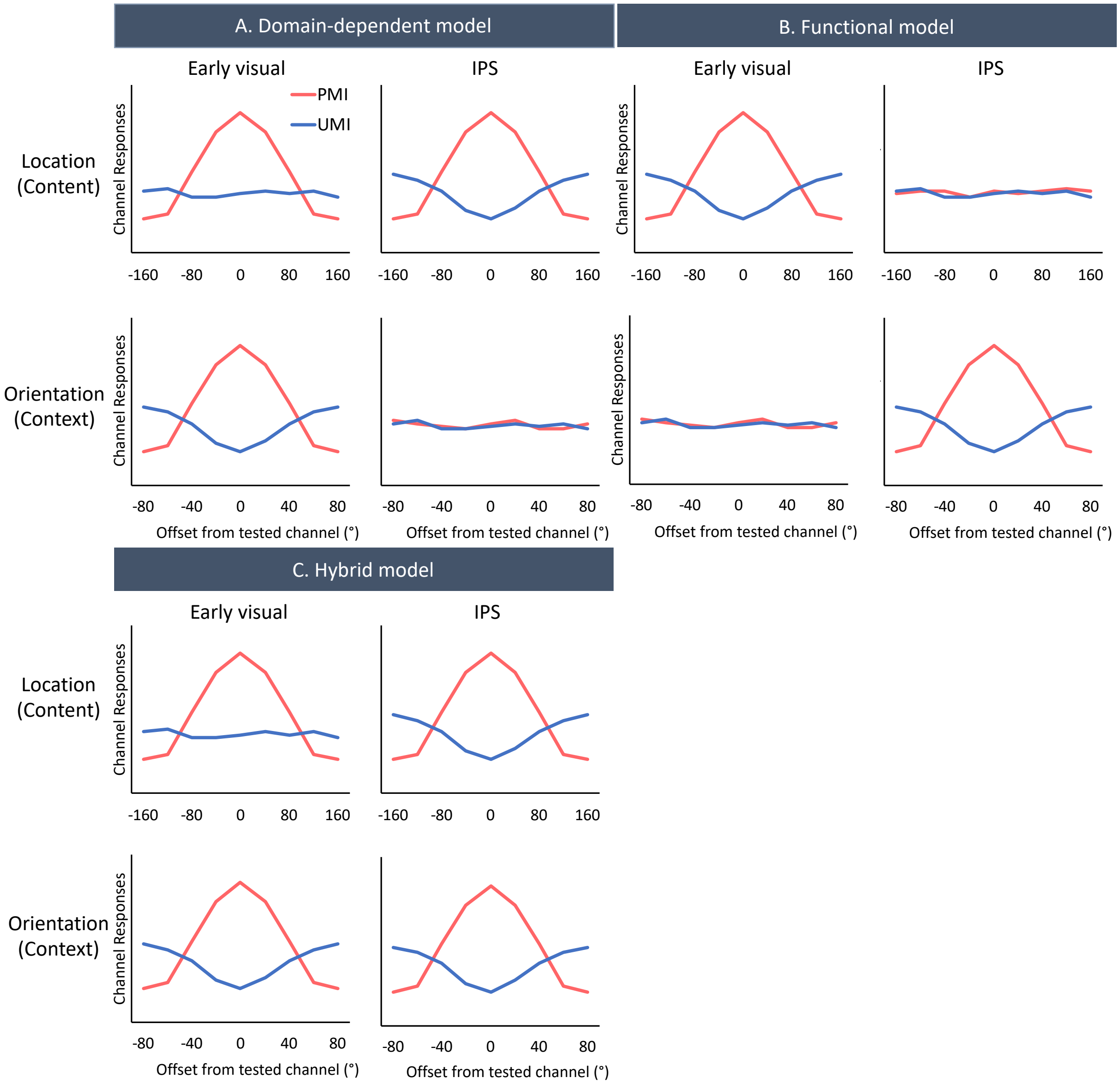

Figure 2. Predictions of location and orientation reconstructions according to the three different models. We consider the opposite patterns between PMI and UMI as evidence for priority-based remapping. A). Domain-dependent model predicts priority-based remapping for orientation in early visual cortex and location in IPS. B). Functional model predicts priority-based remapping for content in early visual cortex and context in IPS. C). Hybrid model predicts domain-dependent priority-based remapping for orientation in early visual cortex and location in IPS, as well as context (orientation) being encoded in IPS.